



Transient electromagnetic interferences between a power line and a pipeline due to a lightning discharge: An EMTP-based approach

Amauri G. Martins-Brito ^{*,[a](#)}, Caio M. Moraes ^a, Felipe V. Lopes ^b

^a University of Brasília, Distrito Federal, Brazil

^b Federal University of Paraíba, Paraíba, Brazil



ARTICLE INFO

Keywords:

ATP
Ground potential rise
Induced voltages
Inductive coupling
Lightning discharges
Pipelines
Soil resistivity
Transmission lines

ABSTRACT

This paper presents a transient electromagnetic interference study in a right-of-way shared between an 88 kV transmission line and a 14" pipeline, with a complex approximation layout based on real project data, and analyses of the induced voltages along the interfered pipeline due to lightning discharges. A circuit model implementation based on the Alternative Transients Program (ATP) with frequency-dependent parameters is built to predict the transient inductive interference effects and ground currents caused by lightning surges. The model is validated using industry-standard software, and then leveraged to perform a detailed investigation of how lightning discharges with different characteristics and how distinct soil properties affect the propagation of the induced voltage wavefronts along the interfered pipeline. Results are expressed in terms of electromagnetic interference (EMI) zones within which the pipeline may be subjected to potentially hazardous voltages.

1. Introduction

Cases of electromagnetic interferences between transmission lines and pipelines sharing the same right-of-ways have become more frequent and complex, due to the increasing industrialization in countries and the environmental regulations becoming more restrictive with respect to the use of space. For this reason, EMI studies involving these facilities have been gaining importance in the literature [1–3].

EMIs may occur when a metallic pipeline is exposed to the energized conductors of a transmission line, which results in unwanted voltages and currents along the interfered system, due to the electromagnetic coupling between the installations involved [3]. The inductive influence of a transmission line conductor on a nearby pipeline depends on the current magnitude, distance between structures, exposure length, soil resistivity, approximation geometry and characteristics of materials [3]. Moreover, in cases of faults involving the ground or lightning strikes into the shield wires, there is current flow to the earth, causing the ground potential rise (GPR) in the vicinities of the power line grounding conductors, which may subject the interfered pipeline to stress voltages due to conductive coupling. As a consequence of EMIs, risks to the integrity of living beings and facilities exposed may appear, such as: touch and step voltages, damage to the insulating coating, to the pipe metal itself and to equipment connected to the pipeline, such as cathodic protection

rectifiers, insulating flanges, telemetry systems etc.

On the other hand, lightning strikes are a recognized source of concern for power line operators, due to the risks of line flashover or insulation failure of transformers, arresters or other equipment, which may ultimately lead to power supply interruption. Besides, in the presence of a neighboring pipeline, potentially hazardous voltages may be transferred to the interfered system, because of the aforementioned electromagnetic coupling mechanisms [4].

Studies based on EMTP-type tools to predict the effects of EMIs have been reported in the literature, with satisfactory results for simple and complex approximation layouts, as well as uniform and multilayered soil models. However, to the best of the authors' knowledge, recent contributions to this field are mostly concerned with: (i) steady-state (harmonic) phenomena in complex interference geometries; or (ii) the transient response caused by lightning discharges involving simpler parallel approximations [5–7].

The authors aim to take the EMTP-based EMI research one step further and investigate the transient coupling effects caused by lightning discharges involving a complex approximation geometry, in which the pipeline exposure to the transmission line is comprised of parallelisms, obliquities and crossing points. This is accomplished by using a modified equivalent circuit model, in which the transmission line and the interfered conductors are modeled and simulated in the same instance,

* Corresponding author.

E-mail addresses: amaurigm@lapse.unb.br (A.G. Martins-Brito), caio.missiaggia@aluno.unb.br (C.M. Moraes), felipe.lopes@cear.ufpb.br (F.V. Lopes).

natively accounting both for the inductive and capacitive coupling mechanisms and accurately obtaining the current distribution along the shield wires and tower grounding electrodes, and with the advantage that the frequency dependence is also considered in the mutual couplings with the interfered conductor, distinguishing from current practices that represent the pipeline by means of cascaded nominal- π (lumped) elements with fixed parameters [3,6,8,9].

This paper presents a case study based on real project data involving a 88 kV power line and a 14'' aboveground pipeline in the southeast of Brazil. First, a quick steady-state analysis is performed with the purpose of validating the circuit model. Then, a lightning discharge is simulated at the transmission line point closest to the pipeline, and transient induced voltages are observed. The effect of the soil is evaluated, with additional simulations considering different resistivity scenarios. Finally, stress voltages caused by the ground potential rise along the pipeline path are analyzed.

Of practical interest to power companies and industries which rely on pipeline transportation systems, this work is expected to contribute with realistic techniques to detect and neutralize risks to which living beings and facilities are subjected, thus aiding in the task of designing safer projects.

2. Mathematical model

2.1. Inductive coupling calculations

The currents flowing through the transmission line energized conductors produce time-varying magnetic fields which, on their turn, cause the rise of electromotive forces (EMFs) in the metallic pipeline following the same right-of-way.

In a system composed of two parallel conductors, shown in Fig. 1, the electromotive force E is expressed in volts as a function (1) of the current I and the mutual impedance Z_{ij} between conductors i and j , given in ohms per unit length by the well-known Carson's equation (2) [10] :

$$E = Z_{ij} \times I, \quad (1)$$

$$Z_{ij} = \frac{j\omega\mu_0}{2\pi} \ln\left(\frac{D'_{ij}}{D_{ij}}\right) + \frac{j\omega\mu_0}{2\pi} \int_0^\infty \frac{2e^{-H\lambda}}{\lambda + \sqrt{\lambda^2 + j\frac{\omega\mu_0}{\rho} - \omega^2\mu_0\epsilon_0\epsilon_r}} \cos(\lambda D) d\lambda, \quad (2)$$

in which I is the source current, in ampères; $\mu_0 = 4\pi \times 10^{-7}$ H/m is the free space magnetic permeability constant; $\epsilon_0 \approx 8.85 \times 10^{-12}$ F/m is the vacuum electrical permittivity; ρ is the soil resistivity, in $\Omega \cdot \text{m}$; ϵ_r is the soil relative permittivity; H , D , D_{ij} and D'_{ij} are the relative distances represented in Fig. 1, in meters, with: $H = |y_i - y_j|$, $D = |x_i - x_j|$, D_{ij} =

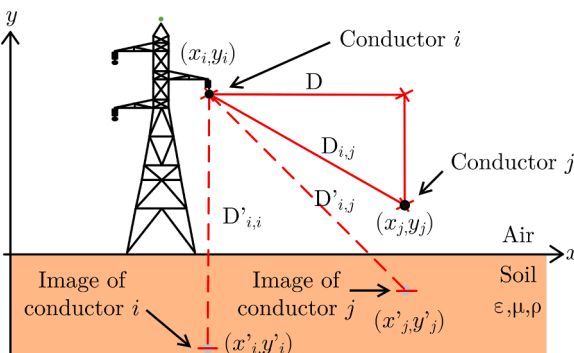


Fig. 1. Overhead conductors and respective images.

$$\sqrt{(x_i - x_j)^2 + (y_i - y_j)^2}$$
 and $D'_{ij} = \sqrt{(x_i - x'_j)^2 + (y_i - y'_j)^2}$.

A widely employed solution to (2) consists of expanding the improper integral in terms of a power series [10]. According to [11], the EMTP/ATP Line Constants routine uses an adaptive technique that parses the geometric and physical problem parameters to find the number of terms necessary for the power series to converge with a discrepancy close to zero with respect to the closed-form solution of Carson's formula (2), yielding accurate results for a broad range of frequencies, resistivities and conductor spacings.

2.2. Capacitive coupling calculations

Capacitive coupling effects are evaluated in terms of the Maxwell potential coefficients and the method of images, which is a reasonable approximation for frequencies up to 1 MHz [3]. Referring again to the system shown in Fig. 1, mutual potential coefficients P_{ij} are determined in m/F according to the following expression:

$$P_{ij} = \frac{1}{2\pi\epsilon_0\epsilon_r} \ln\left(\frac{D'_{ij}}{D_{ij}}\right), \quad (3)$$

in which ϵ_0 is the vacuum electric permittivity, in F/m; ϵ_r is the medium relative electric permittivity; D'_{ij} is the distance between conductor i and the image of conductor j , in meters; and D_{ij} is the distance between conductors i and j , in meters.

2.3. Conductive coupling calculations

Conductive coupling is caused by the injection of current into the soil by a transmission line during phase-to-ground fault conditions or subjected to lightning currents, as illustrated in the simplified model shown in Fig. 2.

Assuming the lightning discharge to be represented by a current source at the soil surface (point P) and that the observation point O is sufficiently apart from point P , the GPR is approximated as [3,12]:

$$\hat{U}(P, O) = \frac{\rho I}{2\pi r}, \quad (4)$$

in which $\hat{U}(P, O)$ is the scalar potential at point O , produced by the source placed at point P , in volts; ρ is the soil resistivity, in $\Omega \cdot \text{m}$; I is the discharge current, in ampères; and r is the euclidean distance between points P and O , in meters.

2.4. Lightning discharge model

The lightning current pulse is described by a peak value, rise time

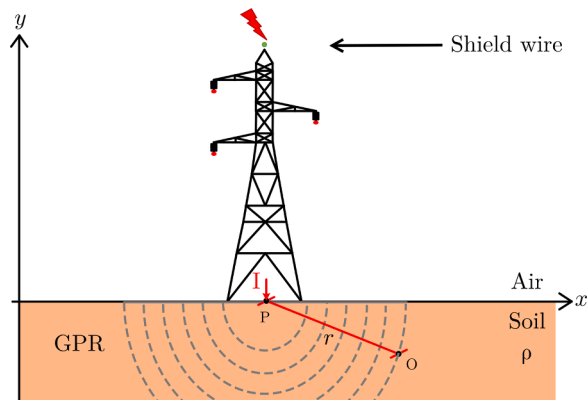


Fig. 2. Simplified model for the GPR around a transmission line tower hit by a lightning discharge.

and half-value time and is expressed by the Heidler function (5) [13]:

$$I_s(t) = \frac{I_0}{\eta} \frac{(t/\tau_1)^n}{1 + (t/\tau_1)^n} e^{(-t/\tau_2)}, \quad (5)$$

in which I_0 is the current amplitude at the base of the lightning channel, in A; τ_1 is the rise time constant, in s; τ_2 is the half-value time constant, in s; n is an integer (1, 2, ..., 10); and η is the current amplitude correction factor, given by:

$$\eta = e^{[(\tau_1/\tau_2)(n\tau_1/\tau_2)]^{-1/n}}. \quad (6)$$

In this paper, lightning strikes with different time constants are evaluated, with rise and half-value times (τ_1/τ_2) of, respectively, 1/50 μ s, 8/20 μ s and 10/350 μ s, which are parameters reported to be critical in lightning studies [14]. Discharge magnitude is 200 kA for all cases. Fig. 3 shows the waveforms of the lightning pulses with such characteristics.

2.5. Equivalent EMTP/ATP circuit model

In order to model the general case, which may be comprised of parallel sections, obliquities and crossings, the pipeline is subdivided in coupling regions and approximated by equivalent parallel exposures, with lengths L_{eq} and distances d_{eq} with respect to the transmission line axis. This subdivision methodology is described in detail in [9].

Then, each coupling region is built in the ATP by using Line/Cable Constants (LCC) objects, as exemplified in Fig. 4, which perform the inductive and capacitive calculations discussed in the preceding sections. Parameters of the transmission line and the pipeline are computed using the J. Martí line model (frequency-dependent parameters) within the range from 60 Hz up to 1 MHz, in order to accurately account for the higher order frequency components present in the waveforms shown in Fig. 3 [15]. Shunt resistors R_G represent the grounding resistance at each tower location and provide the ground currents necessary for GPR computations. Since the interfered installation is aboveground, there is no shunt admittance at the pipeline nodes (i.e. the coating impedance is replaced by an open circuit).

By cascading the necessary number of LCC cells shown in Fig. 4, arbitrary configurations can be built. The lightning model is included by connecting a Heidler type 15 source between the shield wire and the ground at the appropriate line section.

3. Real case study

3.1. System description

The system depicted in Fig. 5 is composed of an untransposed single circuit transmission line, triangular conductor configuration with the side view shown in Fig. 6, operating at 88 kV. In conditions of nominal load, the transmission line is energized with 100 A per phase, with ABC sequence, frequency 60 Hz. Grounding resistances at the terminal

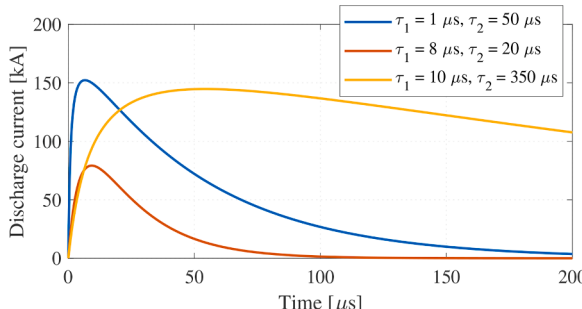


Fig. 3. Lightning discharge waveforms with time constants 1/50 μ s, 8/20 μ s and 10/350 μ s and magnitude 200 kA.

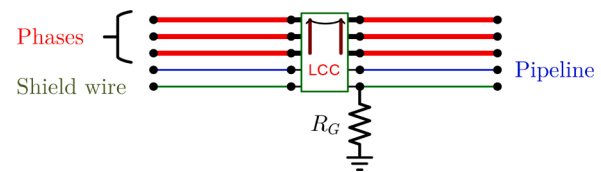


Fig. 4. ATPDraw representation of one section of a three-phase line with one shield wire and one interfered aboveground pipeline.

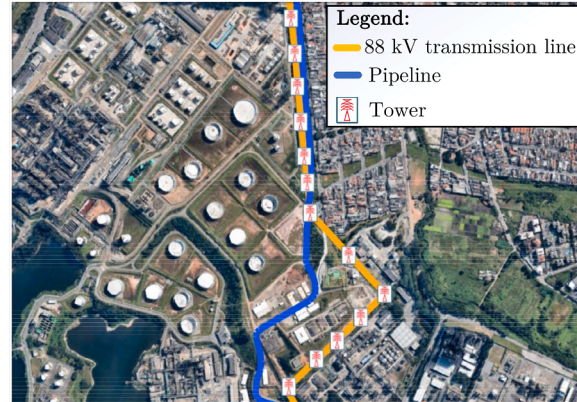


Fig. 5. Top view of the real right-of-way shared between a transmission line and a pipeline.

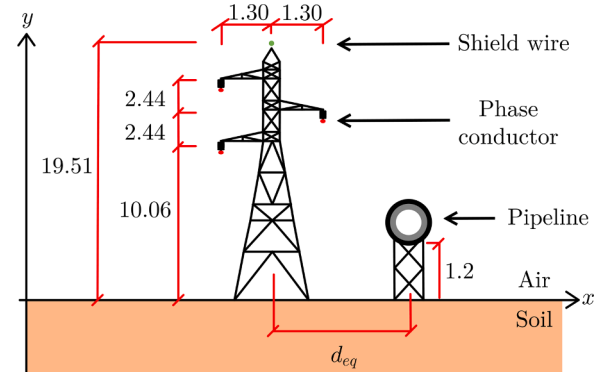


Fig. 6. System side view.

substations are equal to 1 Ω and, at the tower footings, equal to 10 Ω . Table 1 contains the specifications of the transmission line and pipeline conductors.

As Fig. 5 shows, the transmission line shares the space with a pipeline over an extension of approximately 1.2 km. The pipeline is made of carbon steel with a diameter of 14'', positioned aboveground at 1.2 m and it is grounded at the extremities through resistances equal to 10 Ω .

The soil is represented as a uniform structure based on the apparent resistivity measurements described in [5]. Since the objective is to investigate the transient propagation along the interfered pipeline, and not the influence of the soil model, the apparent uniform resistivity value equal to 427.36 $\Omega \cdot \text{m}$ is chosen, which is reported to provide a

Table 1
Specifications of system conductors.

Conductor	External radius [m]	R [Ω/km]	X [Ω/km]
ACSR Grosbeak	0.0125705	0.0924806	0.0156758
Steel 3/8" EHS-CG	0.004572	3.42313	0.261225
Pipe 14"	0.1778	0.099516	0.0990797

conservative inductive coupling scenario [5].

For the reader concerned with the fact that natural soils are layered structures, it is relevant to note that this assumption represents no loss of generality for the purposes of this paper, since, as demonstrated in [16] and [17], there are techniques available to represent models composed of multiple layers in terms of uniform equivalents, which are fully compatible with the EMTP/ATP framework.

3.2. Equivalent circuit representation

Fig. 7 illustrates the EMTP/ATP equivalent circuit of the geometric system shown in Fig. 5. The transmission line within the region of interest contains 13 towers and two terminals, yielding 15 coupling regions with the interfered pipeline. The intersection with the pipeline occurs between towers #7 and #8. The Heidler source is positioned to simulate a lightning discharge occurring at the top of tower #7, which is the closest to the pipeline. Even though only the resulting model is provided here, all the necessary steps to build the equivalent circuit from the approximation geometry shown in Fig. 5, including voltage sources, grounding devices etc., are thoroughly discussed in reference [9].

3.3. Circuit validation

To confirm the validity of the proposed circuit model, the Heidler source is first disconnected and, under nominal load conditions and steady-state regime, the pipeline induced voltages are obtained. Results are shown in Fig. 8 and compared with the software Right-of-Way, widely regarded as the industry-standard for EMI studies [18].

Results agree with the reference values, with an excellent fit at the crossing region and a RMS error of 9.9%, which is mainly explained by the different line models and impedance formulations used in each approach. As the proposed circuit is validated, the next section follows with the simulation of lightning strikes and the transient effects observed in the interfered pipeline.

3.4. Inductive coupling due to lightning discharges

In this section, two analyses are performed. First, the effect of the lightning current waveform is evaluated. Then, additional simulations are carried out for different soil resistivity values.

In all scenarios, plots of the induced voltages along the pipeline are provided, in order to investigate how the inductive coupling waveform propagates through the interfered system.

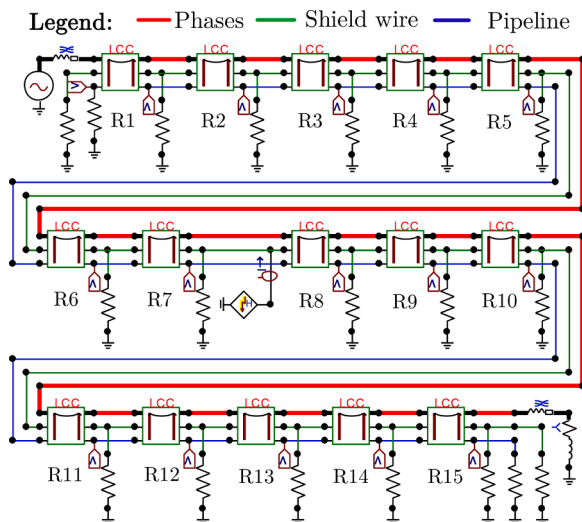


Fig. 7. Equivalent circuit of the system shown in Fig. 5.

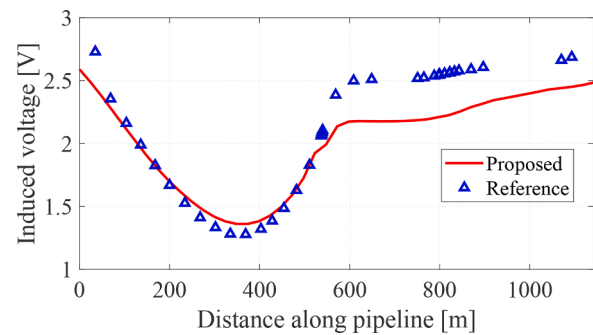


Fig. 8. Pipeline induced voltages in steady-state regime.

3.4.1. Effect of the lightning current waveform

Fig. 9 represents the induced voltage over time at the pipeline point closest to the transmission line (intersection center), for the different current discharges described in Fig. 3. At the most critical point, voltages transferred to the pipeline due to inductive coupling reach the maximum values shown in Table 2 for the corresponding times t_{peak} . Fig. 10 describes how the induced potentials distribute along the pipeline over time.

Observing curve trends in Fig. 10, one may clearly see that the voltage distributions attenuate as the observation point moves away from the pipeline point closest to the lightning discharge. To further investigate this behavior, Table 3 defines three reference values, corresponding, respectively, to 25%, 50% and 75% of the maximum induced values, and Table 4 summarizes how far they occur from the incidence point at $t = t_{peak}$.

To put the practical significance of these results in perspective, one may recall that modern pipeline coatings are designed to withstand a voltage limit of 25 kV [19]. Therefore, for all cases considered, the incidence of a lightning strike in the vicinities of the pipeline, in the absence of appropriate grounding, may cause coating damage within a radius of at least 401 m with respect to the pipeline point closest to the interfering transmission line. In the following section it is investigated how the soil resistivity affects the induced voltage attenuation radius.

3.4.2. Effect of the soil resistivity

Fig. 11 describes the induced voltages over time at the pipeline intersection for different soil characteristics. Simulations consider a lightning pulse with peak value 200 kA, $\tau_1 = 10 \mu s$ and $\tau_2 = 350 \mu s$, with soil resistivities equal to 10 $\Omega \cdot m$, 100 $\Omega \cdot m$ and 1000 $\Omega \cdot m$, covering a wide range of real soils [8]. Fig. 12 presents the voltage distribution along the pipeline for each resistivity scenario considered and different times after the lightning incidence.

One interesting observation is that the voltage distribution along the pipeline does change slightly with the soil resistivity, which is explained by the dependence with terms ω and ρ expressed in (2).

Fig. 12 and Table 5 indicate that pipeline induced voltages increase

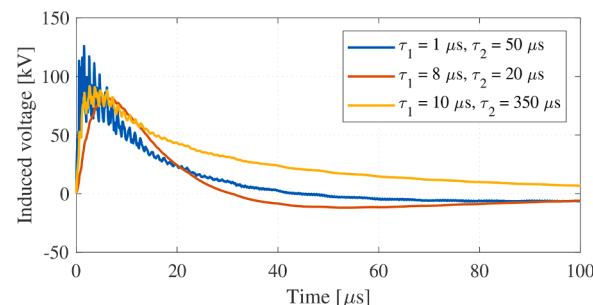
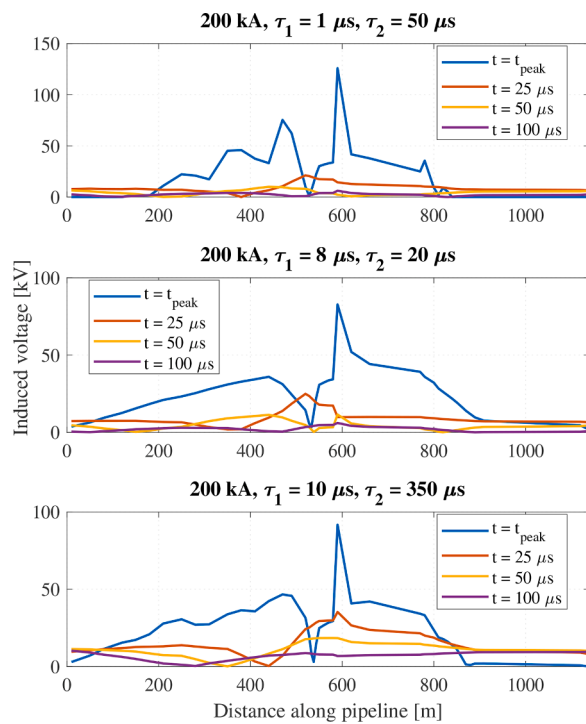


Fig. 9. Pipeline induced voltages at the intersection point for different lightning waveforms.

Table 2

Induced voltage peak values at the closest pipeline point.

Discharge time constants	V_{peak} [kV]	t_{peak} [μ s]
1/50 μ s	125.9	1.542
8/20 μ s	82.75	6.180
10/350 μ s	91.75	1.974

**Fig. 10.** Induced voltages along the pipeline for different discharge current waveforms and times.**Table 3**

Induced voltage reference values for different discharge characteristics.

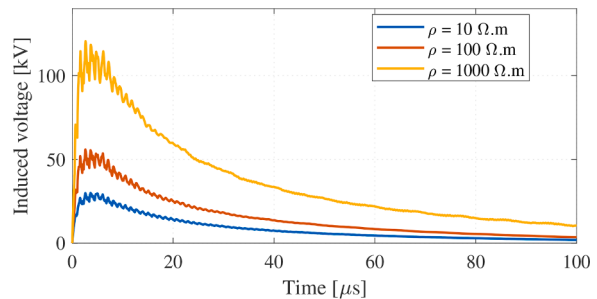
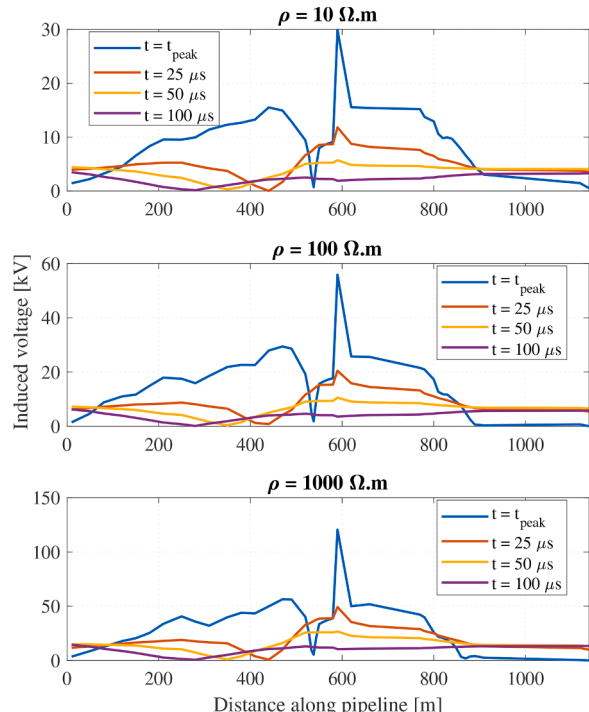
Induced voltage [%]	1/50 μ s	8/20 μ s	10/350 μ s
Absolute value [kV]			
75% of V_{peak}	94.43	62.06	74.48
50% of V_{peak}	62.95	41.38	49.65
25% of V_{peak}	31.48	20.69	24.83

Table 4

Induced voltage attenuation regions for different discharge characteristics.

Induced voltage [%]	1/50 μ s	8/20 μ s	10/350 μ s
Distance from incidence point [m]			
75% of V_{peak}	2.99	3.99	3.99
50% of V_{peak}	100.99	151.99	102.99
25% of V_{peak}	339.99	382.99	400.99

with the soil resistivity, which agrees with previous reports in the literature and is related to the fact that the induced EMF is proportional to the mutual impedance, as (1) shows, which, on its turn, increases with the soil resistivity [5]. This subject is thoroughly discussed in [20], which contains a parametric study describing the ground return impedance sensitivity with respect to the soil resistivity and other variables. On the other hand, with higher resistivity values, the induced

**Fig. 11.** Pipeline induced voltages at the intersection point for a 200 kA, 10/350 μ s lightning strike and different soil resistivities.**Fig. 12.** Induced voltages along the pipeline for a 200 kA, 10/350 μ s lightning strike and different soil resistivities.**Table 5**

Induced voltage reference values for different soil resistivities.

Induced Voltage [%]	10 Ω .m	100 Ω .m	1000 Ω .m
100% of V_{peak}	29.91	55.87	120.51
75% of V_{peak}	22.43	41.90	90.38
50% of V_{peak}	14.96	27.94	60.26
25% of V_{peak}	7.48	13.97	30.13

Table 6

Induced voltage attenuation regions for different soil resistivities.

Induced voltage [%]	10 Ω .m	100 Ω .m	1000 Ω .m
Distance from incidence point [m]			
75% of V_{peak}	3.99	3.99	3.99
50% of V_{peak}	120.99	97.99	94.99
25% of V_{peak}	423.99	379.99	375.99

voltage wavefront attenuates more steeply, affecting narrower pipeline regions. This is verified in the attenuation distances summarized in Table 6.

Defining the EMI region as the radius within which the induced voltage wavefront attenuates to 25% of the initial value, Fig. 13 displays a map view of the potentially unsafe pipeline extensions.

3.5. Ground conduction effects

Under this section, it is presented an investigation of the ground potential rise at the soil surface along the interfered pipeline, caused by the lightning currents flowing through the transmission line ground conductors. Referring back to the geometry shown in Fig. 5, and considering the original case with soil resistivity $427.36 \Omega\text{m}$ and a lightning discharge with 200 kA , $\tau_1 = 10 \mu\text{s}$ and $\tau_2 = 350 \mu\text{s}$ occurring at the top of the tower closest to the pipeline intersection, Fig. 14 describes the ground currents distribution along the transmission line over time.

As Fig. 14 clearly shows, currents propagate from the lightning incidence point towards the line terminals, affecting earth potentials along the pipeline path differently as the time progresses. Since the pipeline is installed aboveground and considered to be ungrounded within the exposure region shown in Fig. 5, there is no potential transfer from the earth to the pipeline metal itself [3]. Nevertheless, if the pipeline conductor is at potential E_T , because of the inductive coupling, and the neighboring soil is at potential U_E , due to conductive coupling (GPR), the resulting open-circuit voltage E_S , expressed in volts according to (7) and known as stress voltage, may give cause to unsafe conditions, as Fig. 15 exemplifies. This is the definition of touch voltage, according to IEEE Std. 80 [21].

$$E_S = E_T - U_E. \quad (7)$$

By using (4), the current values described in Fig. 14 and the superposition theorem, the contributions of all towers to the pipeline GPR are computed. Pipeline inductive components are the same as in Fig. 10, resulting in the stress voltage profiles shown in Figs. 16, 17, 18, 19.

It can be seen that the GPR values are considerably larger in magnitude than the corresponding pipeline voltages caused by inductive coupling phenomena, which is due to the simultaneous current contributions from all towers within the exposure zone, which are amplified by the soil resistivity influence, as a closer inspection of (4) indicates. Therefore, the GPR drives the stress voltage outcome, which agrees with previous reports in the literature [3,4]. Also, it can be seen that the resulting GPR magnitudes concur with recent studies available, which are based on frequency-domain methods [22], as well as time-domain simulations [23]. As the time progresses, GPR and stress voltage curves present new peaks at pipeline points in the close vicinities of the transmission line towers, which agrees with the current behavior shown in Fig. 14. While the phenomena associated with the lightning

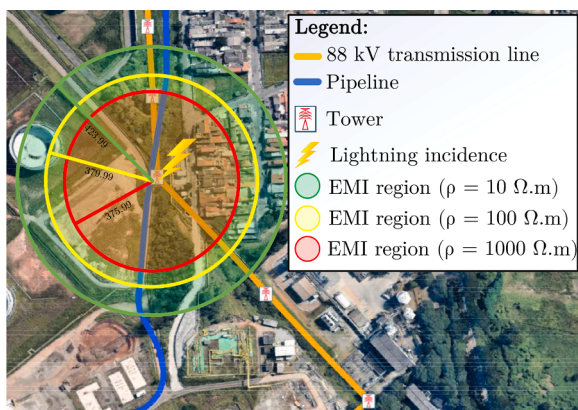


Fig. 13. EMI regions for different soil resistivities.

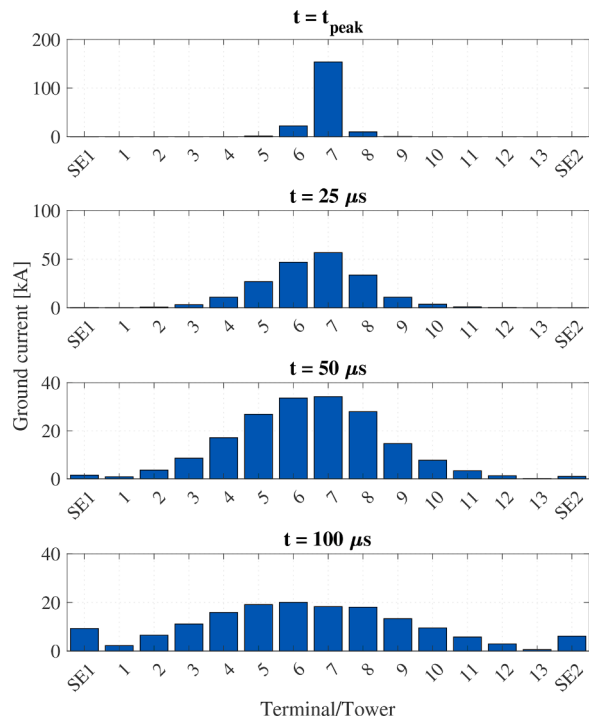


Fig. 14. Currents injected into the soil through the grounding conductors of each tower and substations (SE1 and SE2), for different times.

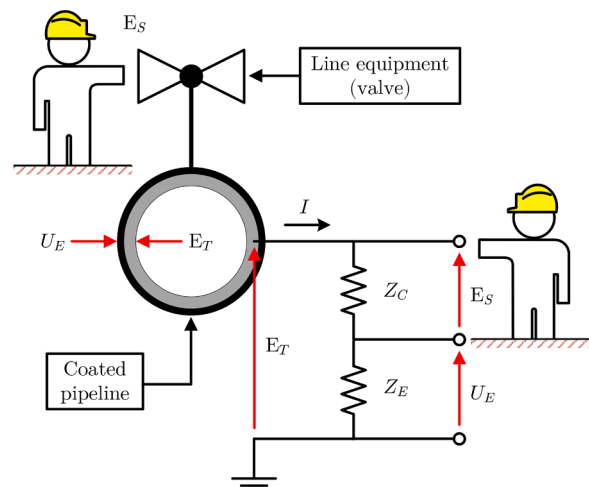


Fig. 15. Illustration of E_S , E_T and U_E and a pipeline operator in contact with the interfered conductor. Z_C and Z_E represent, respectively, coating and earth impedances.

discharge is affecting the pipeline and its surroundings, the resulting stress (or touch) voltages far exceed the safe limits, which calls for mitigation measures, such as the installation of grounding grids at locations accessible to human beings.

4. Conclusions

This work discussed a circuit model based on the EMTP/ATP, devised to predict the effects of transient inductive coupling interferences between a pipeline and a transmission line subjected to a lightning discharge. A case study based on a real pipeline project was performed, with analyses of how the lightning discharge characteristics and the soil resistivity affect the transient induced voltage propagation along the interfered system.

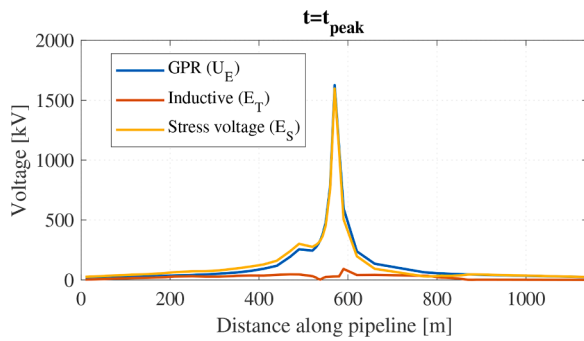


Fig. 16. Pipeline stress voltages for a 200 kA, 10/350 μ s lightning strike and $t = t_{peak}$.

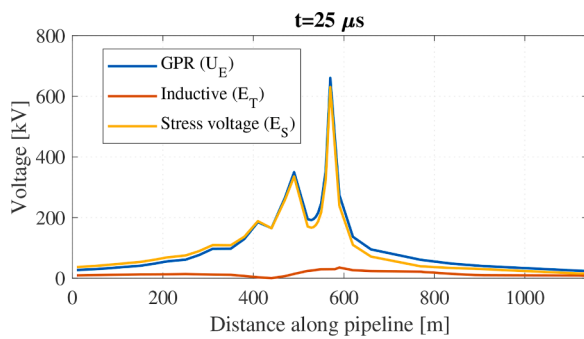


Fig. 17. Pipeline stress voltages for a 200 kA, 10/350 μ s lightning strike and $t = 25 \mu$ s.

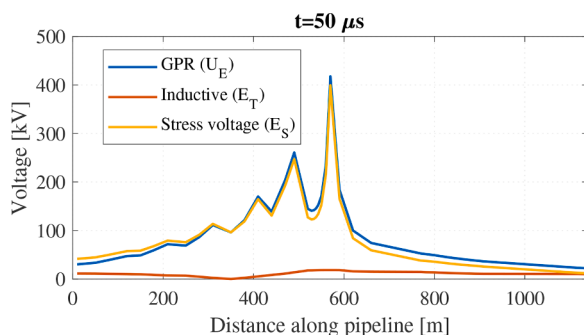


Fig. 18. Pipeline stress voltages for a 200 kA, 10/350 μ s lightning strike and $t = 50 \mu$ s.

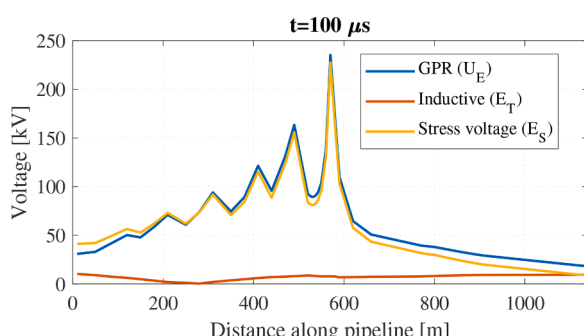


Fig. 19. Pipeline stress voltages for a 200 kA, 10/350 μ s lightning strike and $t = 100 \mu$ s.

It was found that the lightning discharge waveform and the soil resistivity determines both the peak values and the spatial distributions of the transient induced voltages. For different discharge characteristics and a soil resistivity of 427.36 $\Omega\cdot m$, the pipeline regions exposed to potentially hazardous voltages ranged within a radius from 3 m to 401 m with respect to the lightning incidence point. For different soil resistivities and a lightning discharge of 200 kA, 10/350 μ s, the pipeline potentially hazardous zones were found within a radius from 4 m to 376 m. When the conductive coupling response was introduced, considerably larger stress voltage values were found along the entire pipeline path, such that the inductive coupling phenomena became nearly negligible.

This work provided a perspective of how resourceful the EMTP-based EMI simulation techniques can be when applied to real-life problems, especially when one is concerned with the safety of industrial installations. Further research and development of this work will include additional case studies and comparisons with methods based on the electromagnetic theory.

CRediT authorship contribution statement

Amauri G. Martins-Brito: Conceptualization, Methodology, Software, Validation, Formal analysis, Investigation, Writing - original draft, Writing - review & editing. **Caio M. Moraes:** Software, Validation, Formal analysis. **Felipe V. Lopes:** Supervision, Validation, Writing - original draft, Writing - review & editing.

Declaration of Competing Interest

The authors declare that they have no known competing financial interests or personal relationships that could have appeared to influence the work reported in this paper.

References

- [1] L. Qi, H. Yuan, L. Li, X. Cui, Calculation of interference voltage on the nearby underground metal pipeline due to the grounding fault on overhead transmission lines, IEEE Trans. Electromagn. Compat. 55 (5) (2013) 965–974, <https://doi.org/10.1109/TEMC.2013.2240391>.
- [2] G.C. Christoforidis, D.P. Labridis, P.S. Dokopoulos, Inductive interference calculation on imperfect coated pipelines due to nearby faulted parallel transmission lines, Electr. Power Syst. Res. 66 (2003) 139–148, [https://doi.org/10.1016/S0378-7796\(03\)00018-X](https://doi.org/10.1016/S0378-7796(03)00018-X).
- [3] CIGRÉ WG-36.02, Technical Brochure n. 95 - Guide on the Influence of High Voltage AC Power Systems on Metallic Pipelines, 1995.
- [4] A.G. Martins-Brito, S.R.M.J. Rondineau, F.V. Lopes, Power Line Transient Interferences on a Nearby Pipeline Due to a Lightning Discharge. International Conference on Power Systems Transients (IPST 2019), Perpignan, France, 2019.
- [5] A. Martins-Brito, C.M. Moraes, F.V. Lopes, S. Rondineau, Low-frequency Electromagnetic Coupling Between a Traction Line and an Underground Pipeline in a Multilayered Soil, 5th Workshop on Communication Networks and Power Systems (WCNPS 2020), IEEE Xplore, Brasília, Brazil, 2020, pp. 1–6, <https://doi.org/10.1109/WCNPS50723.2020.9263746>.
- [6] G.D. Peppas, M.-P. Papagiannis, S. Koulouridis, E.C. Pyrgioti, Induced Voltage on an Aboveground Natural Gas/Oil Pipeline Due to Lightning Strike on a Transmission Line. 2014 International Conference on Lightning Protection (ICLP), ICLP, Shanghai, China, 2014, pp. 461–467.
- [7] D. Caulker, H. Ahmad, M.S.M. Ali, Effect of Lightning Induced Voltages on Gas Pipelines using ATP-EMTP Program. 2008 IEEE 2nd International Power and Energy Conference, IEEE, Johor Bahru, Malaysia, 2008, pp. 393–398, <https://doi.org/10.1109/PECON.2008.4762506>.
- [8] A.G. Martins-Brito. Realistic Modeling of Power Lines for Transient Electromagnetic Studies, University of Brasília, 2020. Doctoral thesis, <https://repositorio.unb.br/handle/10482/39434>.
- [9] C.M. Moraes, A.G. Martins-Brito, F.V. Lopes, Electromagnetic Interferences Between Power Lines and Pipelines Using EMTP Techniques. 5th Workshop on Communication Networks and Power Systems (WCNPS 2020), IEEE Xplore, Brasília, Brazil, 2020, pp. 1–6, <https://doi.org/10.1109/WCNPS50723.2020.9263746>.
- [10] J.R. Carson, Wave propagation in overhead wires with ground return, Bell System Technical Journal 5 (4) (1926) 539–554, <https://doi.org/10.1002/j.1538-7305.1926.tb00122.x>.
- [11] H.W. Dommel, EMTP Theory book, Microtran Power System Analysis Corporation, 1996.

- [12] S. Sekioka, K. Aiba, S. Okabe, Lightning Overvoltages on Low Voltage Circuit Caused by Ground Potential Rise. International Conference on Power Systems Transients (IPST 2007), Lyon, France, 2007.
- [13] IEC, IEC 61312-1: Protection against lightning electromagnetic impulse - Part 1: General principles, 1995.
- [14] J. Ross, Lightning protection, 1980, <https://doi.org/10.1016/b978-0-408-00424-4.50046-4>.
- [15] L. Ribeiro, G. Cunha, A. Martins-Brito, E. Ribeiro, F. Lopes, Analysis of Traveling Waves Propagation Characteristics Considering Different Transmission Line EMTP Models. 5th Workshop on Communication Networks and Power Systems (WCNPS 2020), IEEE Xplore, Brasília, Brazil, 2020, pp. 1–6, <https://doi.org/10.1109/WCNPS50723.2020.9263723>.
- [16] A.G. Martins-Brito, F. Lopes, S. Rondineau, Multi-layer earth structure approximation by a homogeneous conductivity soil for ground return impedance calculations, *IEEE Trans. Power Delivery* 35 (2) (2020) 881–891, <https://doi.org/10.1109/TPWRD.2019.2930406>.
- [17] D.A. Tsiamitros, G.K. Papagiannis, P.S. Dokopoulos, A.O.L. Arrangement, Homogenous earth approximation of two-Layer earth structures: an equivalent resistivity approach, *IEEE Trans. Power Delivery* 22 (1) (2007) 658–666.
- [18] F.P. Dawalibi, F. Donoso, Integrated analysis software for grounding, EMF, and EMI, *IEEE Comput. Appl. Power* 6 (2) (1993) 19–24, <https://doi.org/10.1109/67.207467>.
- [19] NACE International, *Mitigation of alternating current and lightning effects volume SP0177*, 2007.
- [20] T.A. Papadopoulos, A.I. Chrysochos, C.K. Traianos, G. Papagiannis, Closed-form expressions for the analysis of wave propagation in overhead distribution lines, *Energies* 13 (17) (2020), <https://doi.org/10.3390/en13174519>.
- [21] IEEE, Guide for Safety In AC Substation Grounding, 2013, 10.1109/IEEESTD.2015.7109078.
- [22] F. Madrin, H. Widyaputera, E. Supriyanto, Z. Malek, M. Taib, M. Yasir, Effects of various earth grid configurations on ground potential rise caused by lightning strike, *International Journal on Robotics, Automation and Sciences* 1 (August 2020) (2019) 14–20, <https://doi.org/10.33093/ijoras.2019.1.2>.
- [23] M. Fakhraei, M. Mahmoudian, E.M.G. Rodrigues, Grounding system modeling and evaluation using integrated circuit based fast relaxed vector fitting approach, considering soil ionization, *Applied Sciences (Switzerland)* 10 (16) (2020), <https://doi.org/10.3390/app10165632>.